National Physical Laboratory

Frequency evaluation of UTC(NPL) by NPL-E3Yb+3 for the period MJD 61319 to 61344

National Physical Laboratory

November 4, 2026

The secondary frequency standard NPL-E3Yb+3 and an optical frequency comb were used to evaluate the frequency of UTC(NPL) over a period of 25 days from MJD 61319 to MJD 61344 (6th October 2026 − 31st October 2026). The Yb^+ ion optical clock operation covers 87.53 % of the total measurement period. The result of the evaluation is reported in table 1 and is made using the CCTF 2025 recommended frequency value for the $4f^{14}6s\ ^2S_{1/2} - 4f^{13}6s^2\ ^2F_{7/2}$ unperturbed optical transition in $^{171}Yb^+$: 642 121 496 772 645.18 Hz with a relative standard uncertainty of $u_{\mathrm{Srep}} = 1.7 \times 10^{-16}$ [1].

Table 1: Results of the evaluation of UTC(NPL) by NPL-E3Yb+3

Period of estimation	y(UTC(NPL)− NPL-E3Yb+3)/10^{-16}	u_{A} /10^{-16}	u_{B} /10^{-16}	$u_{\mathrm{A/Lab}}$ /10^{-16}	$u_{\mathrm{B/Lab}}$ /10^{-16}	u_{Srep} /10^{-16}	Uptime
MJD 61319–61344	−11.68	0.011	0.034	0.25	0.59	1.7	87.53 %

1 Measurement configuration

The operation of NPL-E3Yb+3 is described in section 2 of [2]. The electric octupole (E3) transition of $^{171}Yb^+$ was probed with a clock laser at 467 nm, frequency-doubled from 934 nm. The 934 nm laser was prestabilised to a local cavity and then further stabilised to a 1064 nm ultrastable laser [3] via an optical frequency comb. A feedback loop acting on an acousto-optic modulator (AOM) kept the clock laser frequency in resonance with the $^{171}Yb^+$ clock transition. The optical frequency comb was used to measure the 934 nm laser frequency relative to the reference frequency of the comb, which was the unsteered output of the maser HM5. The frequency ratio between NPL-E3Yb+3 and the unsteered frequency from HM5 was therefore evaluated using the comb measurements of the 934 nm light and the AOM frequency corrections. The steered output of HM6 was used to generate UTC(NPL). Note that the steered maser used to generate UTC(NPL) has changed since the previous reported period (MJD 61309 - 61314). The offset between the

steered HM6 signal and unsteered HM5 signal was measured by a TimeTech TIM-10265 phase comparator throughout the measurement period.

2 NPL-E3Yb+3 evaluation

Type A uncertainty

The type A uncertainty u_A is the statistical contribution from the frequency instability of NPL-E3Yb+3. This was estimated based on a white frequency noise component of $1.5{\times}10^{-15}/\sqrt{\tau}$ applied to the duration of the NPL-E3Yb+3 uptime for the evaluation period. This frequency instability is a conservative estimate, based on the Allan deviation of the frequency ratio with the local optical lattice clock NPL-Sr1 measured in November 2024. The probing parameters in November 2024 had a slightly higher QPN-limited instability than the parameters used for the measurement in the period MJD 61319–61344.

Type B uncertainty

The type B uncertainty u_B is the sum in quadrature of the systematic uncertainty of NPL-E3Yb+3 and the uncertainty of the relativistic redshift relative to the conventionally adopted reference potential $W_0 = 62\ 636\ 856.0\ \mathrm{m^2 s^{-2}}$.

The uncertainty evaluation of NPL-E3Yb+3 is described in [2], and the systematic frequency corrections and uncertainty budget for NPL-E3Yb+3 for the period of this report are given in table 2. The geopotential value for NPL-E3Yb+3 is evaluated based on the ion being 1.029(1) m above a reference marker in the floor of laboratory G4-L16. The geopotential of the reference marker in the zero-tide system is taken from [4].

Electric quadrupole shift

Since October 2024, the measurement of the electric quadrupole shift has been simplified and has become more direct. Previously, the E2 transition was probed in 5 alternating magnetic field directions in order to fit the electric field gradient and calculate the electric quadrupole shift in the y-direction, which is the quantisation axis direction used for probing the E3 transition. Changes in optical setups have enabled the direct probing of the E2 in the y-direction, reducing the required number of magnetic fields from 5 to 3, and allowing the direct measurement of the shift without the need for a fit.

The quadrupole shift was measured twice, once before and once after the month of evaluation and the mean value of the shift was taken. Conditions in the trap were demonstrated to have remained stable throughout the month of evaluation, as judged by periodic monitoring of the ion's micromotion.

Relativistic redshift

Until March 2026, the relativistic redshift correction was calculated using the zero-tide system, which does not take into account oscillations due to solid-earth tides. Since September 2026, the correction also includes an additional component calculated as the long-term time average of the oscillations in the mean-tide system. The potential in the mean-tide system is given by:

$$W^{\text{mean-tide}} = W^{\text{zero-tide}} + W_{20} \tag{1}$$

where $W_{20}(\phi) = 0.9722 - 2.8841\sin^2(\phi) - 0.0195\sin^4(\phi)$ and the latitude ϕ at NPL-E3Yb+3 is $\phi_{\text{NPL}} = 51^\circ\ 25'\ 32''$. The additional fractional frequency correction from W_{20} is therefore -8.877×10^{-18}, and the uncertainty is estimated by considering different start and stop dates for the evaluation of the time average.

Trap-induced AC Zeeman shift

Since September 2026, the evaluation of the trap-induced AC Zeeman shift uncertainty has been updated to include contributions from the uncertainty in the static quadratic Zeeman shift coefficients in addition to the magnetic field uncertainties that were previously included.

3 Frequency comparison

Type A uncertainty

The uncertainty $u_{\text{A/Lab}}$ arises mainly from the dead time in the comparison between HM5 and NPL-E3Yb+3, and includes both a deterministic correction due to maser drift and a stochastic contribution (table 3).

The analysis method for these two contributions is described in detail in section 5.2.2 of [5]. The maser HM5 was drifting linearly throughout the measurement period. The deterministic downtime correction was calculated as the difference between the mean of the linear fit to the maser frequency during the uptime of NPL-E3Yb+3 and the mean of the linear fit during the entire measurement period MJD 61319–61344.

The method used to determine the stochastic downtime uncertainty is similar to that described in [6]. The fast Fourier transform of the data validity array is multiplied by the power spectral density calculated from the maser model such that the root mean square fluctuation can be extrapolated to the full evaluation period.

The maser noise model used comprised white phase noise of $2.1\times10^{-13}/\tau$, white frequency noise of $3.8\times10^{-14}/\sqrt{\tau}$, and a flicker frequency floor of 2.0×10^{-16}.

For this evaluation period, NPL-E3Yb+3 had an uptime of 87.53 %, distributed as shown in figure 1.

Table 2: Uncertainty budget for NPL-E3Yb+3 for this evaluation period. Reported uncertainties correspond to 68% confidence intervals. Only leading frequency corrections are shown in this table (corrections or uncertainties $\geq 1 \times 10^{-19}$). This table applies to the period MJD 61319–61344.

Systematic effect	**Correction** $/10^{-18}$	**Uncertainty** $/10^{-18}$
Black-body radiation	0	1.2
Electric quadrupole	−28.1	0.9
Quadratic Zeeman (DC)	29.0	0.6
Background gas collisions	0	0.6
Servo offset	0	0.6
Second-order Doppler	1.8	0.4
Phase chirp	0	0.4
Trap-induced AC Zeeman	−0.3	0.2
AC Stark - probe beam	0	0.2
Quadratic Zeeman (AC)	0.1	0.1
Trapping RF Stark	0.4	< 0.1
Total correction	**2.9**	**2.0**
Relativistic redshift	−1195.8	2.7
Total including relativistic redshift	**−1192.8**	**3.4**

The TimeTech phase comparator that measures the offset between HM5 and UTC(NPL) introduces an additional contribution to $u_{\mathrm{A/Lab}}$, which is computed from the stability of the phase difference of UTC(NPL) referenced to itself with an equivalent TimeTech phase comparator of the same model.

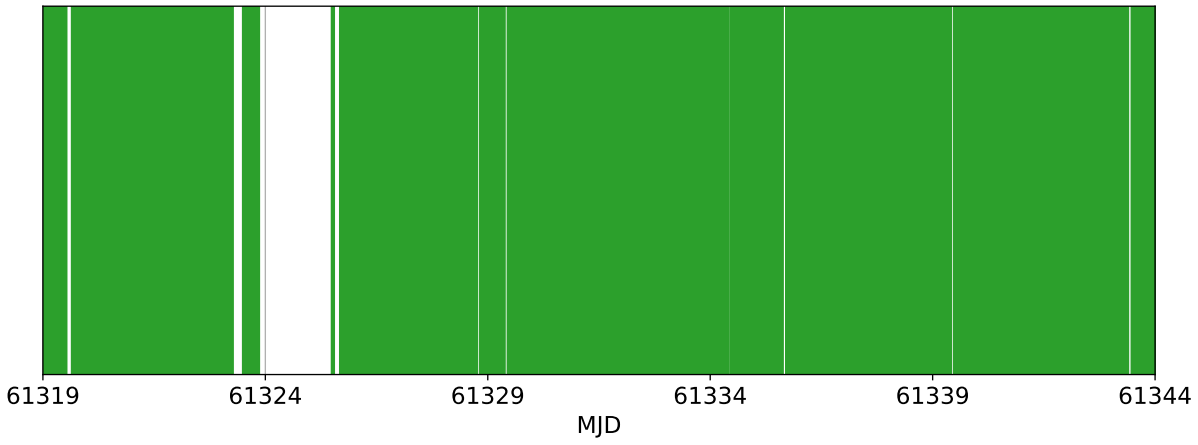


Figure 1: Uptime of NPL-E3Yb+3 over the evaluation period (green regions).

Contribution	Uncertainty / 10^{-18}
$u_{\mathrm{A/Lab}}$[Deterministic]	5
$u_{\mathrm{A/Lab}}$[Stochastic]	24
$u_{\mathrm{A/Lab}}$[HM5-UTC(NPL)]	1
$\boldsymbol{u_{\mathrm{A/Lab}}}$**[Total]**	25

Table 3: A breakdown of the uncertainties included in $u_{\mathrm{A/Lab}}$.

Type B uncertainty

The most significant contribution to the uncertainty $u_{\mathrm{B/Lab}}$ is the distribution of the 10 MHz signal from HM5 to the frequency comb laboratory, and the subsequent synthesis in that laboratory of an 8 GHz signal against which the repetition rate of the frequency comb was measured. Potential phase fluctuations were monitored using a loop-back comparison as described in reference [7], and their contribution to the uncertainty estimated from the instability of these fluctuations over the evaluation period.

The TimeTech phase comparator that measures the offset between HM5 and UTC(NPL) also contributes to $u_{\mathrm{B/Lab}}$. This contribution is estimated based on the long-term instability of the phase difference of UTC(NPL) referenced to itself, measured with an equivalent TimeTech phase comparator of the same model.

Contribution	Uncertainty / 10^{-18}
$u_{\mathrm{B/Lab}}$[Distribution]	59
$u_{\mathrm{B/Lab}}$[HM5-UTC(NPL)]	0.2
$\boldsymbol{u_{\mathrm{B/Lab}}}$**[Total]**	59

Table 4: A breakdown of the uncertainties included in $u_{\mathrm{B/Lab}}$.

References

[1] Bureau International des Poids et Mesures. Recommended values of standard frequencies. https://www.bipm.org/en/publications/mises-en-pratique/standard-frequencies.

[2] A Tofful, C F A Baynham, E A Curtis, A O Parsons, B I Robertson, M Schioppo, J Tunesi, H S Margolis, R J Hendricks, J Whale, R C Thompson, and R M Godun. $^{171}Yb^{+}$ optical clock with 2.2×10^{-18} systematic uncertainty and absolute frequency measurements. *Metrologia*, 61(4):045001, 2024.

[3] M. Schioppo, J. Kronjäger, A. Silva, R. Ilieva, J. W. Paterson, C. F.A. Baynham, W. Bowden, I. R. Hill, R. Hobson, A. Vianello, M. Dovale-Álvarez, R. A. Williams, G. Marra, H. S. Margolis, A. Amy-Klein, O. Lopez, E. Cantin, H. Álvarez Martínez, R. Le Targat, P. E. Pottie, N. Quintin, T. Legero, S. Häfner, U. Sterr, R. Schwarz, S. Dörscher, C. Lisdat, S. Koke, A. Kuhl, T. Waterholter, E. Benkler, and G. Grosche. Comparing ultrastable lasers at 7×10^{-17} fractional frequency instability through a 2220 km optical fibre network. *Nature Communications*, 13(1):212, 2022.

[4] F. Riedel, A. Al-Masoudi, E. Benkler, S. Dörscher, V. Gerginov, C. Grebing, S. Häfner, N. Huntemann, B. Lipphardt, C. Lisdat, E. Peik, D. Piester, C. Sanner, C. Tamm, S. Weyers, H. Denker, L. Timmen, C. Voigt, D. Calonico, G. Cerretto, G. A. Costanzo, F. Levi, I. Sesia, J. Achkar, J. Guéna, M. Abgrall, D. Rovera, B. Chupin, C. Shi, S. Bilicki, E. Bookjans, J. Lodewyck, R. Le Targat, P. Delva, S. Bize, F. N. Baynes, C. F. A. Baynham, W. Bowden, P. Gill, R. M. Godun, I. R. Hill, R. Hobson, J. M. Jones, S. A. King, P. B. R. Nisbet-Jones, A. Rolland, S. L. Shemar, P. B. Whibberley, and H. S. Margolis. Direct comparisons of European primary and secondary frequency standards via satellite techniques. *Metrologia*, 57(4):045005, 2020.

[5] A Tofful. *Advances in performance and automation of a single ytterbium ion optical clock*. PhD thesis, Imperial College London, 2023.

[6] C. Grebing, A. Al-Masoudi, S. Dörscher, S. Häfner, V. Gerginov, S. Weyers, B. Lipphardt, F. Riehle, U. Sterr, and C. Lisdat. Realization of a timescale with an accurate optical lattice clock. *Optica*, 3(6):563–569, 2016.

[7] R. Hobson, W. Bowden, A. Vianello, A. Silva, C. F. A. Baynham, H. S. Margolis, P. E. G. Baird, P. Gill, and I. R. Hill. A strontium optical lattice clock with 1×10^{-17} uncertainty and measurement of its absolute frequency. *Metrologia*, 57(6):065026, Dec 2020.